Efficient electron transport in tetrapod-like ZnO metal-free dye-sensitized solar cells

Wei-Hao Chiu,[a] Chia-Hua Lee,[bc] Hsin-Ming Cheng,[ad] Hsiu-Fen Lin,[d] Shih-Chieh Liao,[d] Jenn-Ming Wu[b] and Wen-Feng Hsieh*[ae]

Received 6th February 2009, Accepted 10th March 2009
First published as an Advance Article on the web 25th March 2009
DOI: 10.1039/b902595m

The tetrapod-like ZnO nanopowders are employed to construct an efficient electron transport network as the photoanode of the dye-sensitized solar cells (DSCs). Due to the high extinction coefficient of the metal-free D149 dye offering a high photocurrent through the ZnO network, the best performance of DSCs based on a 42 μm terapod-like ZnO film showed a high energy conversion efficiency of 4.9% with a high short-circuit photocurrent density of 12.3 mA cm^{-2}, an open-circuit photovoltage of 0.6 V, and a fill factor of 0.65 under AM 1.5 irradiation. Highly efficient electron transport may also be ascribed by a long effective electron diffusion length of 46 μm determined from the electrochemical impedance spectroscopy which is consistent with thickness dependent J_{SC} measurements.

1. Introduction

Dye-sensitized solar cells (DSCs) have received great interest in both basic research and technology development due to their inexpensiveness and capability of large-scale solar energy conversion.[1,2] A power conversion efficiency of the DSCs of more than 10% has been achieved using the TiO_2 nanocrystalline thin film sensitized by ruthenium-based dyes by Grätzel *et al.*[3] Recently, ZnO is another candidate for use in the photoanode of DSCs due to its direct wide-band gap of 3.37 eV and high electron mobility, which is about 17 cm^2 V^{-1} s^{-1} for single-crystal ZnO nanowires.[4] The bandgap and the conduction band energies of ZnO are similar to TiO_2, the common photoanode material, but it has a higher mobility than TiO_2. 1D nanostructures of ZnO, such as nanowires and nanotubes,[5] have been easily achieved to significantly improve the electron transport in the photoanode films by providing a direct conduction pathway for the rapid collection of photogenerated electrons.[6] Jiang *et al.*[7] reported the ZnO nanoflower photoanode *via* a hydrothermal method having 1.9% power conversion efficiency. Martinson *et al.*[8] introduced ZnO nanotube photoanode DSCs by using an anodic aluminum oxide (AAO) method and achieved 1.6% efficiency. However, most of these 1D-nanostructured ZnO-based DSCs have a low current density due to small photoanode surface area with low dye loading so that they exhibit low light harvesting. In our previous study,[9] we reported the branched ZnO nanowires grown by the solvothermal method that can improve the internal surface area of the photoanode to achieve twice the short circuit current as compared with the bare ZnO nanowire ones.

Utilizing sensitized dye with a high absorption coefficient is another approach to enhance the light harvesting. Recently, the metal-free indoline D149 dye was reported by Horiuchi *et al.*[10] which has a high mole absorption coefficient of 68 700 M^{-1} cm^{-1} at 526 nm that is almost five times larger than the ruthenium dye N719 (13 900 M^{-1} cm^{-1} at 541 nm).[11] Hosono *et al.*[12] reported that D149-sensitized DSCs with the ZnO nanosheet photoanode *via* a chemical-bath deposition (CBD) method exhibits 4.2% power conversion efficiency. Moreover, the metal-free dye is not only more environmentally friendly but also cheaper than the ruthenium-based dye and black dye for mass production

[a]*Department of Photonics & Institute of Electro-Optical Engineering, National Chiao Tung University, 1001 Tahsueh Road, Hsinchu, 30050, Taiwan. E-mail: wfhsieh@mail.nctu.edu.tw; Fax: +886 3-5716631; Tel: +886 3-5712121 ext. 56316*
[b]*Department of Materials Science and Engineering, National Tsing-Hua University, Hsinchu, 300, Taiwan*
[c]*Photovoltaics Technology Center, Industrial Technology Research Institute, Hsinchu, 310, Taiwan*
[d]*Material and Chemical Research Laboratories, Industrial Technology Research Institute, Hsinchu, 310, Taiwan*
[e]*Institute of Electro-Optical Science and Engineering, National Cheng Kung University, Tainan, Taiwan*

Broader context

Solar energy is a clean, renewable, and inexhaustible energy source. Dye-sensitized solar cells (DSC) are one of several important photovoltaic (PV) devices in the conversion of solar photon to electrical energy, due to their low cost and easy-handling fabrication. To achieve a highly efficient device, the most important issues should be considered including light harvesting capability and electron transport efficiency. In DSCs, the dye plays a role of collecting and converting solar photons to electrons, so the dye should collect as many photons as possible. Then the generated electrons would further be injected to the semiconductor as the photoanode. The injected electrons can travel through the semiconductor with good electron diffusivity to the external electron collector. This paper describes a concept of DSCs with a novel photoanode structure that adsorbs high extinction dye.

In this paper, we reported that the photoanode film composed by tetrapod-like ZnO nanoparticles, which were fabricated by a novel DC plasma method,[13,14] with D149 dye provides good electron transport and light harvesting to achieve a conversion efficiency as high as 4.9%. And the electron transport properties in ZnO photoanode are also analyzed by the electrochemical impedance spectroscopy (EIS).

2. Experimental section

2.1. Synthesize tetrapod ZnO nanopowders and cell fabrication

In this study, tetrapod-like ZnO nanopowders were synthesized by using a novel DC plasma reactor operated at 70 kW and atmospheric pressure. The synthesis rate of the tetrapod-like ZnO nanopowder can easily reach 1.2 kg h^{-1}. The detailed synthetic procedure and its relative characterizations were discussed in previous studies.[13,14] The ZnO paste for screen-printing was prepared typically by mixing tetrapod-like ZnO powder, ethyl cellulose (EC), and terpineol (anhydrous, #86480, Fluka),[15] and the detailed procedure is as follows. EC (5–15 mPa s, #46070, Fluka) and EC (30–70 mPa s, #46080, Fluka) were dissolved in ethanol to yield 10 wt% solution, individually. 12 g EC (5–15) and 12 g EC (30–70) were added to a round bottomed rotavap flask containing 12 g tetrapod-like ZnO powders, and 25 g terpineol. The mixture paste was dispersed in an ultrasonic bath. And a rotary-evaporator (BUCHI V850) is used to remove the ethanol and water in the mixture paste. Finally, paste was made with a three-roll mill (EXAKT E50).

The dye-sensitized solar cell is basically sandwiched together with many parts. The electrode of photoanode was prepared by screen-printing a 0.28 cm^2 tetrapod-like ZnO film on 3 mm thick fluorine-doped tin oxide glass (FTO, Nippon Sheet Glass Co. Ltd.) with resistance of 7 Ω per square, and no blocking layer was deposited on FTP glass. The photoanode electrode was then gradually heated under an O_2 flow at 400 °C for 60 min to remove the organic materials in the paste. After cooling to room temperature, the ZnO photoanode electrode was immersed into a solution made of 0.5 mM D149 organic sensitizer[10] (Mitsubishi Paper Mills Limited) and 1 mM chenodeoxycholic acid (CDCA, Sigma-Aldrich) in acetonitrile/tert-butyl alcohol mixture (v/v = 1 : 1) at 65 °C for 30 min, and the photoanode electrode was then rinsed with acetonitrile. The counter electrode was also made of NSG FTO glass onto which a nanocrystalline Pt catalyst was deposited by decomposing from H_2PtCl_6 at 400 °C for 20 min. The internal space of the ZnO photoanode electrode and counter electrode was separated by 60 μm thick hot-melting spacer (Surlyn, Dupont), and was filled through a hole with a liquid electrolyte solution which composed of 0.6 M 1,2-dimethyl-3-propylimidazolium iodide (PMII), 0.05 M I_2 (Sigma-Aldrich), and 0.5 M *tert*-butylpyridine (TBP, Sigma-Aldrich) in acetonitrile.

2.3. Sample characterization

The morphologies and dimensions of the tetrapod-like ZnO nanoparticles were characterized using a JEOL-6500 field emission scanning electron microscope (FESEM) operated at 10 KeV. The advanced structures of the tetrapod-like ZnO were analyzed using a JEOL JEM-2100F field emission transmission electron microscope (FETEM) operated at 200 KeV. For current–voltage characteristics and EIS measurements, a white light source (Yamashita Denso, YSS-100A) was used to give an irradiance of 100 mW cm^{-2} (the equivalent of one sun at AM 1.5) on the surface of the solar cell, and the data was collected by an electrochemical analyzer (Autolab, PGSTAT30). The light power was calibrated with a set of neutral density filters using a silicon photodiode (BS-520, Bunko Keiki). The impedance measurements were carried out applying a bias of the open circuit voltage (V_{oc}), namely, under the condition of no electric current. The EIS measurements were recorded in a frequency range from 0.05 Hz to 1 MHz with AC amplitude of 10 mV. The action spectra of the incident monochromatic photon to current conversion efficiency (IPCE) for solar cells were measured with an IPCE measurement system (C-995, PV-measurement Inc.). The UV-visible spectra were measured on a Hitachi U-2800 spectrophotometer.

3. Results and discussion

The quality of photoanode film is an important issue for the performance of the DSCs, due to the condition of the dye absorption and ability of electron transport in the photoanode. Fig. 1(a) shows the SEM image of screen-printing tetrapod-like ZnO film. The tetrapod-like ZnO nanopowders construct a good and dense porous thin film on the FTO substrate by connecting with each other and forming a porous network. The porous network can provide an efficient pathway to transport the photocurrent from the excited dye molecules. Each of the tetrapod-like ZnO nanopowders consists of four crystalline pods with a diameter and a length of about 30 nm and 100–400 nm, respectively. Surface area of the tetrapod-like ZnO nanopowders is about 10 m^2 g^{-1} from the BET measurement. Further examinations of the crystalline quality of the tetrapod-like ZnO powders were performed with FETEM as shown in Fig. 1(b). The high resolution FETEM image shows each arm of the tetrapod ZnO was preferentially oriented in the c-axis direction with the single-crystal wurtzite structure, and the distance between lattice planes was measured to be 5.2 Å corresponding to the lattice constant of ZnO (002) plane, which is the same as a single crystalline nanowire. After 400 °C necking, the electrons can travel from one tetrapod unit to the neighborhood unit *via* the interface electron hopping mechanism as the DSCs with the photoanode made of TiO_2 nanoparticles so that the electron

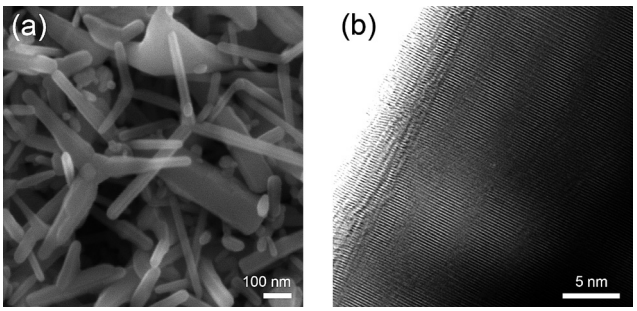

Fig. 1 (a) The FESEM images of the tetrapod-like ZnO nanopowder after screen-printing on FTO glass, (b) the FETEM image of an arm of tetrapod-like ZnO.

diffusion driving force in the porous film only depends on the film thickness d.[16,17] Thus, the high crystalline ZnO tetrapods can improve the electron transport in the porous network.

In order to improve the DSCs' performance, it is important to optimize the thickness of the porous photoanode layer, because the photovoltaic characteristics significantly depend on the thickness of the porous photoanode. In this study, the thickness of the tetrapod-like ZnO photoanode were varied from 5 μm to 42.2 μm, and the photovoltaic characteristics of the DSCs' performance can be seen in Fig. 2. First, the open-circuit voltage (V_{OC}) decreases linearly with the increase of ZnO film thickness (Fig. 3(a)). The V_{OC} is the difference of the electron Fermi levels of the photoanode and the electrolyte, so the behavior of V_{OC} is suggested by an inhomogeneous density of the light in the porous ZnO film to contribute an inhomogeneous electron Fermi level of photoanode. In Fig. 2(b), the filling factor (FF), which is the ratio of the maximum power to the product of maximal V_{OC} and short-circuit photocurrent density (J_{SC}) affected by the series resistance of the cell, keeps almost a constant of 0.65 with increasing the ZnO film thickness to 42.2 μm. On the other hand, the series resistance of the cell, which includes the resistance of FTO, photoanode, electrolyte, and Pt counter electrode, may not change too much with the thickness of photoanode due to the low resistance of the high crystalline ZnO tetrapod network. And it also indicates that the tetrapod ZnO network exhibits efficient electron transport for such thick ZnO photoanodes. The J_{SC} is increasing with the thickness of tetrapod-like ZnO film in contrast with the V_{OC}, because a greater photoanode surface area with thicker film is obtained to enhance the dye loading and the photocurrent. However, the J_{SC} does not increase linearly with the increase of ZnO film thickness because the larger surface area of the photoanode also has more recombination sites. The maximal J_{SC} is obtained presently with 42.2 μm thick film from Fig. 2(c). It is therefore important to note that the optimization of photoanode thickness by using tetrapod-like ZnO is about twice as thick as that by using ZnO nanosheet structure photoanode.[12] Finally, the energy conversion efficiency of the solar cells can be calculated by

$$\eta = \frac{V_{OC} J_{SC} FF}{P_{in}}$$

where P_{in} is the optical power of 100 mW cm^{-2} under AM 1.5. From the above results, the magnitude of the variation of both V_{OC} and FF is smaller than that of J_{SC}. Therefore, the energy conversion efficiency (η) is dominated by J_{SC} as shown in Fig. 2(d). The energy conversion efficiency has a peak value of 4.9% for our 42.2 nm thick DSC.

From the above results, the 42.2 μm tetrapod-like ZnO dye-sensitized solar cell with D149 and CDCA absorption shows a good photovoltaic performance and the photocurrent–voltage (I–V) curve is shown in Fig. 3(a). The photovoltaic characteristics are comparable to the previous literature[12] with J_{SC}, V_{OC}, FF, and the efficiency being 12.4 mA cm^{-2}, 607 mV, 0.65, and 4.9%, respectively. The high photocurrent density is attributed to

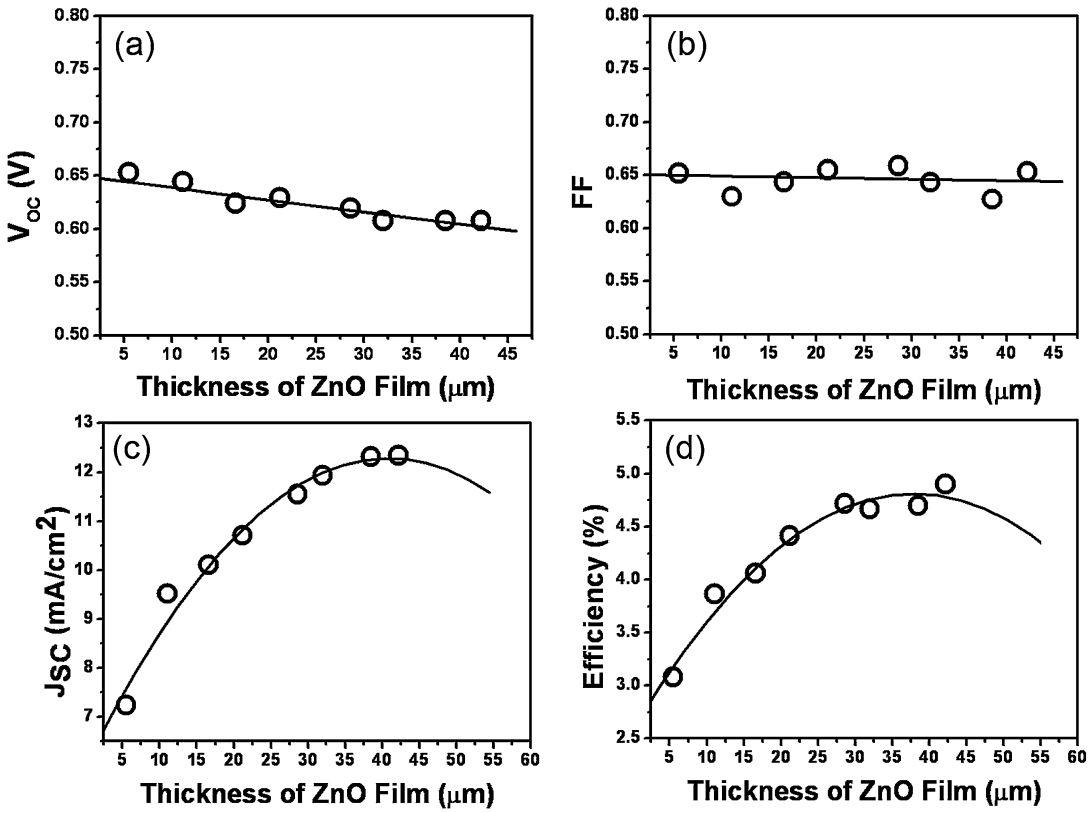

Fig. 2 Thickness dependent photovoltaic characteristics of the tetrapod-ZnO DSCs with D149 dye. (a) Open-circuit photovoltage, V_{OC}; (b) Fill factor, FF; (c) Short-circuit photocurrent density, J_{SC}; and (d) Energy conversion efficiency, η. A strong correlation of J_{SC} and η is found. The lines are plotted to guide the eyes.

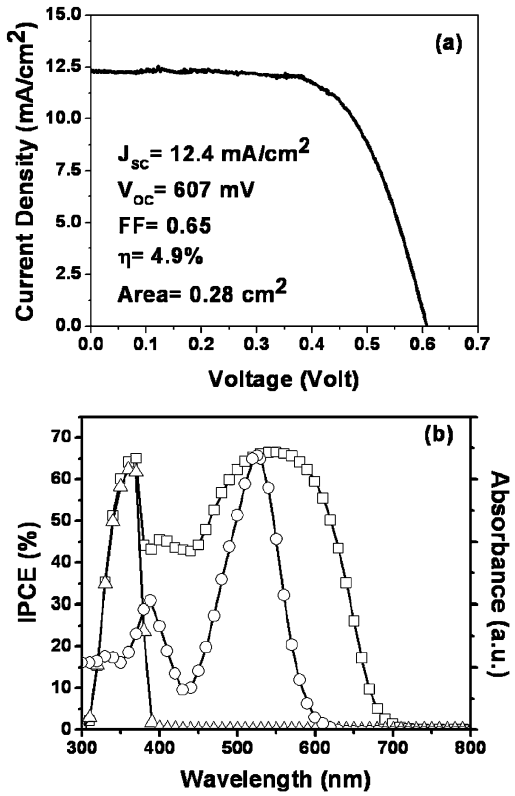

Fig. 3 (a) Photocurrent-voltage curve obtained with DSCs based on D149 and CDCA absorption under AM 1.5 radiation (100 mW cm^{-2}). (b) Absorption spectra of D149 in acetonitrile (-○-) and the spectra of incident photon-to-current conversion efficiencies for 42 μm tetrapod-like ZnO DSCs with D149 and CDCA absorption (-□-) and without any absorption (-△-). The electrolyte was a mixture of 0.5 M PMII, 0.03 M I_2, and 0.5 M TBP in acetonitrile.

the good electron transport in ZnO porous network and the high absorption coefficient of the D149 dye. The absorbance of D149 in acetonitrile (open circles) showns in Fig. 3(b) revealing peaks at 526 and 388 nm. Here, the IPCE for the cells with D149 and CDCA absorption (open squares) reaches more than 60% in the spectral range from 490 nm to 600 nm that is contributed from the D149 absorption peak of 526 nm; whereas, the absorption peak of D149 at 388 nm contributes more than 40% to IPCE in the range from 390 nm to 450 nm. The IPCE spectra of D149 dye and CDCA adsorbed on ZnO film (after 400 nm) is similar to pure D149 absorption spectra in solution but exhibits a red shift and peak broadening due to the interaction of the anchoring carboxyl group to the ZnO surface, and the results indicates that the excited electron can transport efficiently through the porous ZnO network and a large photocurrent is also obtained. On the other hand, the other IPCE peak around 370 nm mainly results from the exciton absorption of the ZnO photoanode, because the IPCE of the cells without absorption dye (open triangles) reveal almost the same peak.

The electrical impedance spectroscopy (EIS) is widely used to investigate the characteristics of the photoanode electrode, the electrolyte, and Pt counter electrode in DSC devices, especially the parameters of electron transport in the photoanode electrode.[18] In this study, the EIS measurement is also employed to analyze the performance of the tetrapod porous network photoanode, and the Nyquist Cole–Cole plot of the 42.2 μm tetrapod-like DSCs is shown in Fig. 4(a). The plotted data is analyzed and fitted by using the equivalent electric circuit model. The equivalent electric circuit shown in Fig. 4(b) is the same as our previously study,[9] where R_w is the electron transport resistance from inside the ZnO photoanode, R_k is the charge-transfer resistance related to recombination of electrons, C_μ is the chemical capacitance of the ZnO electrode, R_s is the transport resistance of FTO and external circuits, Z_N is the finite Warburg impedance in the electrolyte, R_{Pt} and C_{Pt} are the charge-transfer resistance and the capacitance at the Pt surface, R_{FTO} and C_{FTO} are the charge-transfer resistance and the interfacial capacitance at the FTO/electrolyte interface, R_{FZ} and C_{FZ} are the resistance and the capacitance at the FTO/ZnO interface, τ_n, D_{eff}, and L_n are the effective electron lifetime, diffusion coefficient, and diffusion length of ZnO photoanode, respectively. The fitting results were summarized in the inset of Fig. 4(a). The effective electron diffusion coefficient in the photoanode (D_{eff}) is calculated by using the relation:[18] $D_{eff} = (R_k/R_w)(L^2/\tau_n)$, where L is the thickness of the tetrapod-like ZnO film. The D_{eff} of 42.2 μm tetrapod-like ZnO DSC is 1.533 × 10^{-3} cm^2 s^{-1} which is much larger than that of TiO_2-based DSCs (1 × 10^{-5} cm^2 s^{-1}).[18] And the effective electron diffusion length for the 42.2 μm tetrapod-like ZnO DSCs is estimated by relation: $L_n = (D_{eff} \times \tau_n)$, to be 45.57 μm. It means the optimal thickness of photoanode is around 46 μm that is consistent with the results of the thickness dependent J_{SC} measurement. The series resistance estimated from EIS fitting is 30.2 Ω *via* the well-known relation[19] indicating

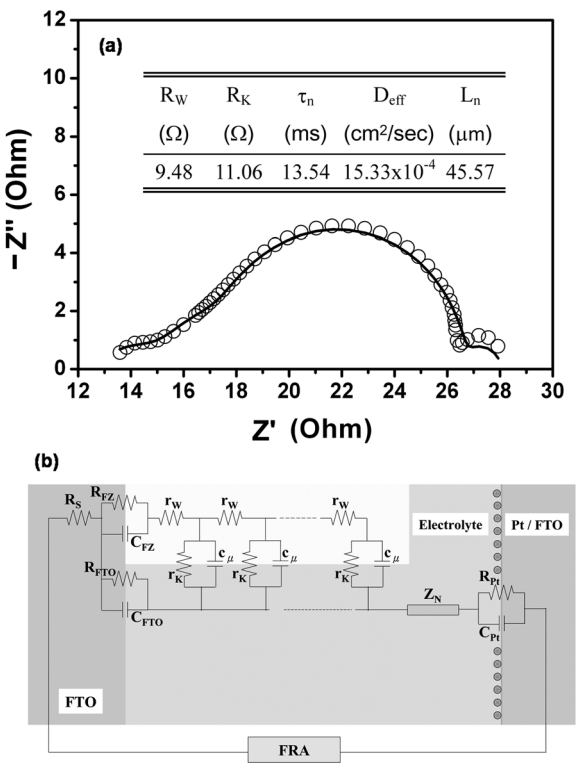

Fig. 4 Nyquist plot of the 42.2 μm tetrapod-like DSCs. The empty circles in (a) are the measurement data points, and the solid curve is the fitting result based on the equivalent circuit model as shown in (b).

consistent with 28.9 Ω calculated from the I–V curve of Fig. 3(a) with the equation of $R_S = (dV/dI)_{I=0}$

The electron collection is one of the most important issues to make a high efficiency cell. Here, a trade-off solution to optimize the electron transport properties and the photoanode surface area is given, and the high energy efficient ZnO-based DSCs with efficient electron collection is also demonstrated. On the other hand, the good conductivity tetrapod ZnO photoanode is easy to make mass production with a screen-printing method or doctor-blade method, in contrast to other 1D nanostructure photoanodes. And the concept of tetrapod structure powder is also suitable to other semiconductor photoanode in DSCs for future applications.

4. Conclusion

In summary, by using the tetrapod-like ZnO porous network as the photoanode the D149 dye-sensitized solar cells are found to exhibit high-performance. The photovoltaic characteristics are greatly affected by the thickness of the tetrapod-like ZnO photoanode, and the optimized thickness of the D149-sensitized tetrapod-like ZnO photoanode is 42.2 μm with conversion efficiency of 4.9% at present, due to the good electron transport ability of ZnO tetrapod network. The good electron diffusion properties with $D_{eff} = 1.53 \times 10^{-3}$ cm^2 s^{-1} and $L_n = 46$ μm are also estimated by the electrochemical impedance spectroscopy.

Acknowledgements

The authors acknowledge the financial support from the National Science Council (NSC) of Taiwan (Project No. NSC96-2628-M-009-001-MY3) and Material and Chemical Research Laboratories (MCL/ITRI) (Project No. 8301XSY4X1) in Taiwan.

References

1 B. O'Regan and M. Grätzel, *Nature*, 1991, **353**, 737–740.
2 B. J. Christophe, F. Arendse, P. Comte, M. Jirousek, F. Lenzmann, V. Shklover and M. Grätzel, *J. Am. Ceram. Soc.*, 1997, **80**, 3157–3171.
3 M. Grätzel, *Inorg. Chem.*, 2005, **44**, 6841–6851.
4 Z. Fan, D. Wang, P. C. Chang, W. Y. Tseng and J. G. Lu, *Appl. Phys. Lett.*, 2004, **85**, 5923–5925.
5 H. Yu, Z. Zhang, M. Han, X. Hao and F. Zhu, *J. Am. Chem. Soc.*, 2005, **127**, 2378–2379.
6 M. Law, L. E. Greene, J. C. Johnson, R. Saykally and P. Yang, *Nat. Mater.*, 2005, **4**, 455–459.
7 C. Y. Jiang, X. W. Sun, G. Q. Lo, D. L. Kwong and J. X. Wang, *Appl. Phys. Lett.*, 2007, **90**, 263501.
8 A. B. F. Martinson, J. W. Elam, J. T. Hupp and M. J. Pellin, *Nano Lett.*, 2007, **7**, 2183–2187.
9 H. M. Cheng, W. H. Chiu, C. H. Lee, S. Y. Tsai and W. F. Hsieh, *J. Phys. Chem. C*, 2008, **112**, 16359–16364.
10 T. Horiuchi, H. Miura, K. Sumioka and S. Uchida, *J. Am. Chem. Soc.*, 2004, **126**, 12218–12219.
11 M. K. Nazeeruddin, S. M. Zakeeruddin, R. Humphry-Baker, M. Jirousek, P. Liska, N. Vlachopoulos, V. Shklover, C. H. Fischer and M. Grätzel, *Inorg. Chem.*, 1999, **38**, 6298–6305.
12 E. Hosono, Y. Mitsui and H. Zhou, *Dalton Trans.*, 2008, 5439–5441.
13 H. F. Lin, S. C. Liao and S. W. Hung, *J. Photochem. Photobiol., A*, 2005, **174**, 82–87.
14 T. S. Ko, S. Yang, H. C. Hsu, C. P. Chu, H. F. Lin, S. C. Liao, T. C. Lu, H. C. Kuo, W. F. Hsieh and S. C. Wang, *Mater. Sci. Eng., B*, 2006, **134**, 54–58.
15 S. Ito, T. N. Murakami, P. Comte, P. Liska, C. Grätzel, M. K. Nazeeruddin and M. Grätzel, *Thin Solid Films*, 2008, **516**, 4613–4619.
16 D. Vanmaekelbergh and P. E. de Jongh, *J. Phys. Chem. B*, 1999, **103**, 747–750.
17 A. L. Roest, P. E. de Jongh and D. Vanmaekelbergh, *Phys. Rev. B*, 2000, **62**, 16926.
18 M. Adachi, M. Sakamoto, J. Jiu, Y. Ogata and S. Isoda, *J. Phys. Chem. B*, 2006, **110**, 13872–13880.
19 Q. Wang, S. Ito, M. Grätzel, F. Fabregat-Santiago, I. Mora-Seró, J. Bisquert, T. Bessho and H. Imai, *J. Phys. Chem. B*, 2006, **110**, 25210–25221.

